ISTITUTO DI ANALISI DEI SISTEMI ED INFORMATICA
CONSIGLIO NAZIONALE DELLE RICERCHE

A. Bertuzzi, A. d'Onofrio, A. Fasano, A. Gandolfi

MODELLING CELL POPULATIONS WITH SPATIAL STRUCTURE: STEADY STATE AND TREATMENT-INDUCED EVOLUTION OF TUMOUR CORDS

R. 578 Novembre 2002

Alessandro Bertuzzi – Istituto di Analisi dei Sistemi ed Informatica del CNR, viale Manzoni 30 - 00185 Roma, Italy. Email : bertuzzi@iasi.cnr.it.

Alberto d'Onofrio – European Institute of Oncology, Division of Epidemiology and Biostatistics, Via Ripamonti 435 - 20141 Milano, Italy. Email : alberto.d'onofrio@ieo.it.

Antonio Fasano – Dipartimento di Matematica "U. Dini", Università di Firenze, viale Morgagni 67/A - 50134 Firenze, Italy. Email : fasano@math.unifi.it.

Alberto Gandolfi – Istituto di Analisi dei Sistemi ed Informatica del CNR, viale Manzoni 30 - 00185 Roma, Italy. Email : gandolfi@iasi.cnr.it.

This work was partially supported by CIMAB, Italy, by the Progetto Strategico CNR "Metodi e Modelli Matematici nello Studio dei Fenomeni Biologici", and by the National Research Project "Problemi a Frontiera Libera", co-financed by MIUR.

ISSN: 1128–3378

Collana dei Rapporti
dell'Istituto di Analisi dei Sistemi ed Informatica, CNR

viale Manzoni 30, 00185 ROMA, Italy

tel. ++39-06-77161
fax ++39-06-7716461
email: iasi@iasi.rm.cnr.it
URL: http://www.iasi.rm.cnr.it

Abstract

Abstract. Tumour cells growing around blood vessels form structures called tumour cords. We review some mathematical models that have been proposed to describe the stationary state of the cord and the cord evolution after single-dose cell killing treatment. Whereas the cell population has been represented with age or maturity structure to describe the cord stationary state, for the response to treatment a simpler approach was followed, by representing the cell population by means of the cell volume fractions. In this latter model, where transport of oxygen is included and its concentration is critical for cell viability, some constraints to be imposed on the interface separating the tumour from the necrotic region have a crucial role. An analysis of experimental data from untreated tumour cords, which involves modelling by cell age and by volume fractions, and some results about the cord response to impulsive cell killing, are also presented.

Key words: Cell populations, tumour cord, nonlinear systems of differential and integral equations, free boundary problems.

1. Introduction

The structure of the vascular system that supplies a tumour is in general complex and irregular, so it is difficult to study the relationship between the distance from blood vessels and the cell proliferation, and therefore between the extent of vasculature and the rate of tumour growth. In some tumours, however, it is possible to observe cylindrical arrangements of viable tumour cells around blood vessels, and this kind of symmetry simplifies the investigation. These structures are named *tumour cords* [31,19,28,29,20]. The cords are generally surrounded by regions of necrosis, since the oxygen tension and the concentration of nutrients such as glucose decay radially within the cord and, when they fall below some critical values, cell death occurs. Tumour cells arranged around vessels of the host, and surrounded by host tissue, have also been observed as a characteristic form of micrometastases [22] and in the initial growth of tumours involving the cooption of host vessels [21]. When necrosis is present, the mean thickness of the cords (*i.e.*, the distance between the vessel wall and the first layer of necrotic cells) has been found to be 60–130 μm in different tumours, whereas the mean radius of the central vessel has been found to be 10–40 μm. As a consequence of the cell proliferation within the cord, outward directed cell migration occurs. The proliferation, as quantified by the fraction of cells in S phase and the fraction of cells in mitosis measured after cell labelling with tritiated thymidine, appears to slow down from the vessel wall to the periphery of the cord [31,19,28]. Also this reduced proliferation is likely to be related to the decrease of the concentration of oxygen, nutrients, and/or other critical chemicals. The response of tumour cords to a single dose of radiation or drugs was investigated in [32,26,27,16]. The general pattern of the response in these experiments showed a regression of the cord radius followed by a regrowth phase towards the unperturbed value.

The spatial distribution of the proliferating cells (represented as a population with age structure) and of the quiescent cells in a tumour cord, was studied by mathematical modelling in [3] and [33]. The model describes the stationary state in the case in which the fraction of newborn cells that become quiescent is a given function of the distance from the blood vessel. The dependence of the progression rate through the cell cycle on the distance from vessels was also investigated, by representing the cell cycle as a sequence of maturity compartments [5] or by means of continuous maturity [15]. The growth of an isolated tumour cord within the normal tissue has been analyzed in [8,9] and in [4]: these models use a quite elementary representation of the tumour cell population but include the diffusion and consumption of the nutrient. A mathematical model for investigating the dynamics of tumour cords under the influence of cell killing agents was proposed in [6]. The existence of a unique stationary state in the absence of therapy was established, as well as the existence and uniqueness of the solution of the evolutive problem that arises when the action of treatment is considered. The response to a single dose of radiation or anticancer drug was extensively investigated by numerical computation of the solutions [7].

In the present paper we give a review of our work in modelling tumour cords. In section 2, the use of structured cell population models to describe the stationary state of a tumour cord is outlined. The model developed to represent the time evolution of tumour cords as a consequence of treatments [6] is described in section 3. In this model, the cell population is simply represented by the fraction of volume occupied by the cells, but the role of oxygen in modulating cell proliferation and maintaining cell viability is included. Results concerning the stationary state and the evolution following the treatment are reported in sections 4 and 5. Together with results already published, here we present a detailed analysis of experimental data concerning the tumour cords of the untreated hepatoma 3924A [28]. This analysis is based on

the models of sections 2 and 3. Moreover, explicit formulas that characterize the cord response are given in the limit case of impulsive cell killing, under further simplifying assumptions.

2. The cell population structure in a tumour cord

In a first attempt to model the cell population within a tumour cord, the population of proliferating cells was structured by age in order to represent the position of cells in the cell cycle and thus the different cycle phases [3]. We give here a brief description of that model.

It was assumed that the tumour cord has cylindrical symmetry, r_0 denoting the radius of the central blood vessel, r the radial distance from the axis of the vessel, and ρ_N the cord radius (see Fig. 1). Cords were considered to be surrounded by necrosis, so that ρ_N identifies the cord/necrosis interface. Experimental observations in untreated tumours suggest that the radius of the interface between the cord and the necrosis is constant with the time. Thus the cord was assumed to have ρ_N constant, and the model was focussed on the stationary state. All the variables describing the cord were assumed to be independent of the axial coordinate.

The population of viable tumour cells was considered as composed by proliferating (cycling) cells and quiescent cells. The population of the cycling cells is described by the cell density $n(a,r,t)$, $n(a,r,t)\,da$ being the number of cycling cells with age between a and $a+da$, in the unit volume, at position r and time t. For the quiescent cells, $n_Q(r,t)$ gives the number of quiescent cells in the unit volume at position r and time t. Assuming that the cell population is in a stationary state, the cell densities will be time-independent functions. Cell motion within the cord was assumed to be radially directed and was represented at the stationary state by a single velocity field $u(r)$ common to all the cells, independently of cell age and of the proliferating or quiescent status. Thus, rearrangements among cell subpopulations due to cell motions of diffusive type were excluded. The total cell density was assumed constant, in view of measurements of the number of cells in histological sections of untreated tumour cords, pointing out that the cell density remains rather unchanged from the inner to the outer regions of the cord [27,28,29].

The effect of microenvironment on cell cycle was represented by assuming that the different concentrations of oxygen and/or nutrients, experienced by the cells as they move within the cord, affect only the transition to quiescence. Since, in a steady state condition, the concentration profile of chemicals will not change with the time, the dependence of cell cycle parameters on such concentrations leads to a dependence of the parameters on the radial distance. Thus we assumed that a fraction $\theta(r) \in [0,1]$ of the cells born at position r enters the cycle, and a fraction $1-\theta(r)$ will become quiescent. All proliferating cells were instead assumed to traverse the cycle in the same time T_c, and thus we have $0 \le a \le T_c$. In view of the observed decrease of the proliferation along the cord radius, the fraction θ will be a nonincreasing function of r. Moreover, the recruitment of quiescent cells into the cycle was considered to be negligible in the untreated cords. All cells die at $r=\rho_N$, and the possible random cell death within the cord was initially neglected.

According to the assumptions previously stated, the conservation equations for the cell densities in the cord at the stationary state, $n(a,r)$ and $n_Q(r)$, can be written as

$$\frac{\partial n}{\partial a} + \frac{1}{r}\frac{\partial}{\partial r}(run) = 0 \tag{1}$$

$$n(0,r) = 2\theta(r)n(T_c,r) \tag{2}$$

$$\frac{1}{r}\frac{d}{dr}(run_Q) = 2(1-\theta(r))n(T_c,r)\,. \tag{3}$$

In Eqs. (2) and (3), $n(T_c,r)$ yields the rate of cell division in the unit volume at distance r. A rigorous determination of cell motion should take into account the mechanical interactions among cells and with the extracellular fluid [2,10,23]. The study of the internal stresses and of the dynamics of the interstitial fluid can be circumvented, however, by the assumption that the total cell density is constant along the radius. In this case, the velocity field u can be easily obtained. By integrating Eq. (1) with respect to age, and taking into account (2) and (3), we have that the total cell density $n_C(r)$

$$n_C(r) = n_P(r) + n_Q(r) = \int_0^{T_c} n(a,r)\,da + n_Q(r)\,, \tag{4}$$

where $n_P(r)$ is the density of proliferating cells at distance r, satisfies the equation

$$\frac{1}{r}\frac{d}{dr}(run_C) = n(T_c,r)\,. \tag{5}$$

Assuming $n_C(r) = n^\star$, the cell densities can be normalized to this constant value. Let $\phi(a,r) = n(a,r)/n^\star$ and $f_Q(r) = n_Q(r)/n^\star$. Since there is no cell flux across the vessel wall, and thus $u(r_0) = 0$, from (5) it follows that

$$ru(r) = \int_{r_0}^{r} r'\phi(T_c,r')\,dr'\,. \tag{6}$$

We note that u is positive, unless $\phi(a,r) \equiv 0$, and thus the cells move towards the periphery and the necrotic region is continuously fed by cells that die when crossing the interface ρ_N. Taking into account Eq. (6), ϕ and f_Q will satisfy the following equations:

$$\frac{\partial\phi}{\partial a} + \frac{1}{r}\frac{\partial}{\partial r}\Big(\int_{r_0}^{r} r'\phi(T_c,r')\,dr'\cdot\phi\Big) = 0 \tag{7}$$

$$\phi(0,r) = 2\theta(r)\phi(T_c,r) \tag{8}$$

$$\frac{1}{r}\frac{d}{dr}\Big(\int_{r_0}^{r} r'\phi(T_c,r')\,dr'\cdot f_Q\Big) = 2(1-\theta(r))\phi(T_c,r). \tag{9}$$

The functions $f_P(r) = \int_0^{T_c}\phi(a,r)\,da$ and $f_Q(r)$ are the fractions of cycling cells and, respectively, of quiescent cells at position r.

The existence and uniqueness of the solutions of equations (7)-(9) has been established by Webb [33]. The condition $\theta(r_0) > 1/2$ is necessary to have a nonzero $\phi(a,r)$ and appears to be biologically meaningful, since it states that there exists a portion of the cord (at least close to the vessel) in which cell division originates a number of proliferating cells larger than the number of quiescent cells.

In the above model, the occurrence of cell death within the cord can also be considered. A small percentage of dead cells (less than 10%) has been found indeed by Moore *et al.* [28]. To account for cell death we may introduce a subpopulation of dead cells, $n_N(r)$ being the number of dead cells per unit volume at distance r, and we assume that dead cells disappear by disgregation according to a rate constant μ_N. The total cell density, $n_C(r)$, is now given by the

right-hand-side of Eq. (4) plus $n_N(r)$, and we still take the total cell density constant and equal to $n^\star$. Thus, the conservation laws can be written as

$$\frac{\partial \phi}{\partial a} + \frac{1}{r}\frac{\partial}{\partial r}(ru\phi) = -\mu_P(a,r)\phi(a,r) \tag{10}$$

$$\phi(0,r) = 2\theta(r)\phi(T_c,r) \tag{11}$$

$$\frac{1}{r}\frac{d}{dr}(ruf_Q) = 2(1-\theta(r))\phi(T_c,r) - \mu_Q(r)f_Q(r) \tag{12}$$

$$\frac{1}{r}\frac{d}{dr}(ruf_N) = \int_0^{T_c} \mu_P(a,r)\phi(a,r)\,da + \mu_Q(r)f_Q(r) - \mu_N f_N(r)\,, \tag{13}$$

where $f_N(r)=n_N(r)/n^\star$ is the fraction of dead cells at position r, and $\mu_P(a,r)$ and $\mu_Q(r)$ are the death rate constants of proliferating and, respectively, quiescent cells. By integrating Eq. (10) with respect to age, and then adding (12) and (13), we obtain for the velocity u the expression

$$ru(r) = \int_{r_0}^{r} r'[\phi(T_c,r') - \mu_N f_N(r')]\,dr'\,. \tag{14}$$

Because of the occurrence of cell death within the cord and the successive disappearance of dead cells, the positivity of the velocity field up to ρ_N, which is a natural requirement in the stationary state of a cord surrounded by necrosis, is no longer guaranteed. Suitable constraints have so to be imposed on T_c, $\theta(r)$ and the loss rates.

The assumption that the cell cycle time is not affected by changes in the microenvironment can be relaxed by describing the cell cycle in terms of cell maturity [30], *i.e.*, in terms of the position of the cell in the cell cycle. In [5], the cycle of tumour cells is described by a sequence of M discrete compartments of cell maturity, so the proliferating cell population in the tumour cord is represented by the functions $n_k(r,t)$, $k=1,\cdots,M$, $n_k(r,t)$ being the number of cells in the k-th compartment in the unit volume at distance r and time t. Under the assumption that the number of cells in the unit volume is constant, let $f_k(r)=n_k(r)/n^\star$ be the fraction of cells in the k-th compartment of maturity at distance r in the stationary state. Assuming Poisson exit from each compartment, together with the possibility of cell arrest in a quiescent status after mitosis, the conservation equations can be written as

$$\begin{aligned}
\frac{1}{r}\frac{d}{dr}(ruf_1) &= 2\theta\lambda_M f_M - \lambda_1 f_1 \\
\frac{1}{r}\frac{d}{dr}(ruf_k) &= \lambda_{k-1}f_{k-1} - \lambda_k f_k\,, \quad k=2,\cdots,M \\
\frac{1}{r}\frac{d}{dr}(ruf_Q) &= 2(1-\theta)\lambda_M f_M\,,
\end{aligned} \tag{15}$$

where λ_k denotes the exit rate constant from the k-th compartment. From the assumption that the number of cells in the unit volume is constant, for the velocity field we have

$$ru(r) = \int_{r_0}^{r} r'\lambda_M(r')f_M(r')\,dr'\,. \tag{16}$$

As for the fraction θ, also the exit rate constants λ_k's may be functions of r, thus making the progression through the cycle dependent on the radial position of the cell. Because of the decay

of oxygen and nutrient concentrations as r increases, these rate constants will be nonincreasing with r. We observe, however, that the stochastic model underlying the equations in (15) has an exponentially distributed residence time in each maturity compartment, so that Eqs.(15)-(16) describe a population with cell-to-cell variability of the cycle transit time even if the exit rates λ_k's are independent of r. Existence and uniqueness of the solutions of Eqs. (15)-(16) was proved in [5].

The representation of the population by a continuous maturity has been considered by Dyson *et al.* [15]. In that paper, the population of proliferating cells is described by a density $n(x, r, t)$, $x \in [0, 1]$ being the cell maturity in the cycle, and the maturation rate is a function of cell maturity and radial distance. Also in this model, aimed at the description of the stationary state, the cell velocity field has been determined by imposing that the number of cells per unit volume does not change with r. The existence and uniqueness of the steady-state solution has been proved. We notice that the age-structured model (1)-(3), in which the cell cycle duration is constant, can be rewritten in terms of maturity by defining $x = a/T_c$ and taking the constant maturation rate $1/T_c$. In this way, it is a particular case of the model in [15].

Instead of assuming that the number of cells per unit volume is constant, we may suppose that the volume fraction occupied *locally* by the cells is constant within the cord, which also leads to the determination of the velocity field $u(r)$. This volume fraction will be smaller than one because an extracellular space, filled by the extracellular matrix and liquids, is present in the tissue. The cells have different volumes according to their position in the cycle or possibly to their quiescence, so the mean cell volume may change with r and a constant local cell volume fraction is not necessarily equivalent to a constant cell density n_C. Assuming the cell volume fraction constant with r, has the physical meaning that the system is arranged according to a uniform "optimal" packing of cells. Let $\nu_C(r)$ denote the cell volume fraction at the stationary state. In the simpler case in which there is no cell death within the cord we can express $\nu_C(r)$ in terms the age structured model (1)-(3), obtaining

$$\nu_C(r) = \int_0^{T_c} v(a) n(a, r)\, da + v(0) n_Q(r) \tag{17}$$

where $v(a)$ is the volume of a proliferating cell of age a, with $v(T_c) = 2v(0)$, and the volume of quiescent cells is assumed equal to $v(0)$. The ratio $\nu_C(r)/n_C(r)$ gives the mean cell volume at the position r. By integrating with respect to age Eq. (1) multiplied by $v(a)$, and adding Eq. (3) multiplied by $v(0)$, the following equation for $\nu_C(r)$ can be written:

$$\frac{1}{r}\frac{d}{dr}\left(ru\nu_C\right) = \int_0^{T_c} \frac{dv}{da} n(a, r)\, da\,. \tag{18}$$

If $\nu_C(r)$ is assumed to be constant and equal to $\nu^\star$, from Eq. (18) it follows that

$$ru(r) = \frac{1}{\nu^\star} \int_{r_0}^{r} r' \int_0^{T_c} \frac{dv}{da} n(a, r')\, da\, dr' \tag{19}$$

and, in the simple case of $v(a) = v_0 + (v_0/T_c)a$,

$$ru(r) = \frac{v_0}{T_c \nu^\star} \int_{r_0}^{r} r' \int_0^{T_c} n(a, r')\, da\, dr'\,. \tag{20}$$

Equations (19) or (20) should now be substituted to Eq. (6) in Eqs. (1)-(3) in order to compute the cell densities $n(a,r)$ and $n_Q(r)$. These densities will be normalized to $\nu^\star/v(0)$, *i.e.*, to the maximal number of cells that can be contained in the unit volume when the cell volume fraction is equal to $\nu^\star$. The expression of the cell volume fraction might also be obtained when the cell population is structured by maturity, by writing the cell volume as a function of cell maturity. Therefore, assuming $\nu_C(r)$ constant, a new expression for the velocity field could similarly be derived.

We note that, if cell volume is linearly increasing with age, the mean cell volume of proliferating cells is equal to $v_0(1+\langle a\rangle/T_c)$, where $\langle a\rangle$ is the mean cell age. It can be easily seen that the mean cell volume in the cord will be always between v_0 (all cells quiescent) and $v_0/\ln 2$ (all cell proliferating). Therefore, under the hypothesis of constant number of cells per unit volume, $\nu_C(r)$ should decrease with r, but the ratio between the cell volume fractions in the outer and the inner region of the cord cannot be smaller than $\ln 2$. These considerations suggest that the assumptions of constant $\nu_C(r)$ or constant $n_C(r)$ could lead in many cases to similar results, despite the different expressions of the velocity field.

Models that incorporate the cell cycle structure are useful to analyze experimental data from labelling experiments designed to investigate how the cell proliferation changes at different distances from the blood vessel [31,19,28]. Examples of these analyses are reported in [3] and [5], where the curves of the labelling index and of the fraction of labelled mitoses at different radial distances were simulated by the proposed models and compared to experimental data.

However, the above models are not able to explain why the stationary radius of the cord attains a particular value, or how the kinetic parameters of the cell population change with the radial distance. To this aim, it is necessary to consider the transport within the cord of the chemicals (oxygen and/or nutrients) that are critical for cell viability and are related to cell proliferation.

3. A model for the treatment-induced evolution of tumour cords including oxygen transport

A mathematical model aimed at describing the evolution of a tumour cord following cytotoxic treatments, and including oxygen transport, was proposed by Bertuzzi *et al.* [6]. In that model, the ideal case of a regular array of tumour cords which are parallel and identical is considered, so that the attention can be focussed on one of them, by supposing that the cord is surrounded by a surface which, because of symmetry, prevents any exchange of matter with the neighboring cords. Because of the complexity of the dynamical problem, a simplified representation of the cell population was chosen, disregarding the cell age and the structure of cell cycle. Three components in the cord and in the necrotic region are distinguished: viable tumour cells, dead cells and extracellular fluid. Dead cells in the cord cannot now be disregarded because of the action of treatment. Only the volume fractions occupied locally by these components are considered: the fractions are denoted as ν_V, ν_N and, respectively, ν_E (with $\nu_V+\nu_N+\nu_E=1$). In the cord it will be $\nu_V>0$, whereas in the surrounding necrotic zone only dead cells and extracellular fluid will be present and $\nu_V=0$. Viable cells, dead cells and extracellular fluid are assumed to have equal mass densities. The treatment is supposed not to affect the tumour vasculature.

As in the models of the previous section, cylindrical symmetry is assumed, cell velocity is radially directed and is the same for both living and dead cells, and all the variables describing the cell population, the cell velocity and the concentrations of chemicals are independent of the

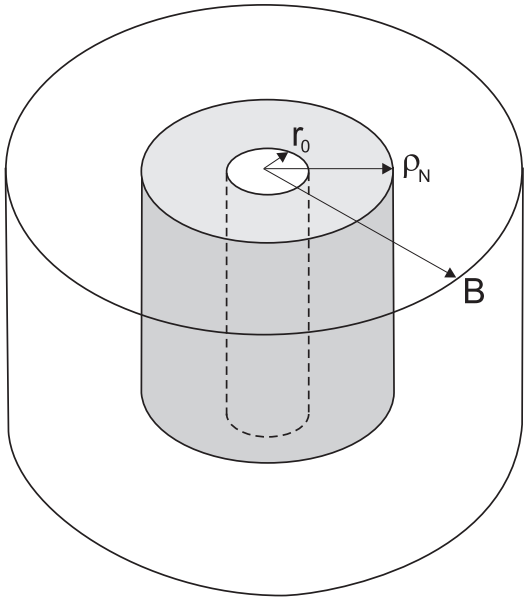

Fig. 1. Geometry of the tumour cord (symbols explained in the text).

axial coordinate. The radius of the external boundary that isolates the cord will be denoted by $B(t)$ (see Fig. 1). In addition, the following assumptions are made: *(i)* Oxygen is the only species of "nutrient" considered and we do not distinguish the intracellular from the extracellular concentration. We denote by $\sigma(r,t)$ the local oxygen concentration. The consideration of only one species of nutrient is common to most of the mathematical models of tumour growth [17,24,1,12,14,10]. *(ii)* We define a rate of cell proliferation, χ, such that $\chi\nu_V$ gives the rate of increment of the volume fraction of viable cells. This rate is a nondecreasing function of σ, $\chi(\sigma)$. More precisely, for σ larger than a given threshold σ_P the cells are fully proliferating and $\chi(\sigma)=\chi_0$. Below σ_P, the progression through the cell cycle slows down and/or the fraction of quiescent cells increases, so that $\chi(\sigma)$ is decreasing. Below σ_Q ($\sigma_Q<\sigma_P$) all cells become quiescent and $\chi(\sigma)=0$. If σ increases over σ_Q, all cells resume instantaneously the proliferative status. *(iii)* Cells die if σ falls to a critical low value σ_N ($\sigma_N<\sigma_Q$). In addition, random cell death, either spontaneous and induced by treatments, may occur within the cord. *(iv)* The rate of spontaneous cell death is a non-increasing function of σ, $\mu(\sigma)$. *(v)* Dead cells are degraded to a fluid waste at a rate μ_N within the cord and at a rate $\tilde{\mu}_N$ in the necrotic region. These possibly different decay rates may be related with different death mechanisms (apoptosis *vs.* necrosis).

We note that the change of χ with σ (and thus its decrease with r) in the model we are discussing corresponds to the decrease of θ with r in model (1)-(3), and to the decrease of the maturation rate with r in the maturity-structured models described in the preceding section.

Similarly to the approach followed in the models described in section 2, the cell velocity is determined on the basis of the assumption: *(vi)* the cell volume fraction $\nu_C=\nu_V+\nu_N$ is constant both in the cord and in the necrotic region. This is now a severe simplification, since *(vi)* is assumed to hold even in the presence of the perturbations generated by the treatment-induced cell death. However, it has a rather clear physical meaning: the system of cells keeps the same packing during any perturbation.

We denote by P, T, and Q the regions of the cord in which $\chi=\chi_0$, $0<\chi<\chi_0$, and $\chi=0$, respectively, and by N the necrotic region. Also, we introduce for the spontaneous cell death

rate $\mu(\sigma)$ a threshold $\sigma_\mu \leq \sigma_P$, above which $\mu(\sigma) = \mu_0 \geq 0$, and let it be $\chi_0 > \mu_0$. We suppose that σ is a known constant $\sigma^\star > \sigma_P$ at the wall of the blood vessel. Thus there is an inner region of the cord in which both the proliferation and spontaneous death rates are constant. The functions $\chi(\sigma)$ and $\mu(\sigma)$ are piecewise continuously differentiable in $[\sigma_N, \sigma^\star]$ with bounded first derivatives. In addition, $\chi'(\sigma) > 0$ for $\sigma \in (\sigma_Q, \sigma_P)$, and $\mu' < 0$ only in some interval $(\bar{\sigma}_\mu, \sigma_\mu)$ with $\sigma_\mu > \bar{\sigma}_\mu \geq \sigma_N$.

Denoting the cell velocity and the velocity of the extracellular fluid by the vectors $\mathbf{u}$ and $\mathbf{w}$ respectively, the mass balance for each of the components in the region $P \cup T \cup Q$ leads to the equations

$$\frac{\partial \nu_V}{\partial t} + \nabla \cdot (\mathbf{u}\, \nu_V) = \chi(\sigma)\nu_V - [\mu(\sigma) + \mu_C(c,\sigma) + \mu_R(\sigma,t)]\, \nu_V \,, \tag{21}$$

$$\frac{\partial \nu_N}{\partial t} + \nabla \cdot (\mathbf{u}\, \nu_N) = [\mu(\sigma) + \mu_C(c,\sigma) + \mu_R(\sigma,t)]\, \nu_V - \mu_N \nu_N \,, \tag{22}$$

$$\frac{\partial \nu_E}{\partial t} + \nabla \cdot (\mathbf{w}\, \nu_E) = -\chi(\sigma)\nu_V + \mu_N \nu_N \,. \tag{23}$$

In writing (21) we have supposed that the proliferation rate is independent of ν_E; this is reasonable if ν_E does not become too small. In Eqs. (21)-(22), $\mu_C(c,\sigma)$ is the death rate induced by a chemical agent whose concentration is $c(r,t)$, while $\mu_R(\sigma,t)$ represents the action of radiation. It is well known that the radiation effect depends on the oxygen level, whereas the dependence on t not only accounts for the treatment schedule, but is also related to the fact that the cell killing effect persists for some time after the radiation pulse [11]. Both μ_C and μ_R are assumed to be twice continuously differentiable, and $\mu_C(0,\sigma) = \mu_R(\sigma,0) = 0$. In the necrotic region the balance equations reduce to

$$\frac{\partial \nu_N}{\partial t} + \nabla \cdot (\mathbf{u}\, \nu_N) = -\tilde{\mu}_N \nu_N \,, \tag{24}$$

$$\frac{\partial \nu_E}{\partial t} + \nabla \cdot (\mathbf{w}\, \nu_E) = \tilde{\mu}_N \nu_N \,. \tag{25}$$

Total mass conservation is obtained by considering that $\nu_V + \nu_N + \nu_E = 1$:

$$\nabla \cdot [\mathbf{u}(\nu_V + \nu_N) + \mathbf{w}\nu_E] = 0 \,, \tag{26}$$

the latter equation emphasizing the presence of a divergence-free compound velocity.

It can be shown that oxygen transport is largely dominated by diffusion and that it is quasi-steady (*i.e.*, it proceeds through equilibrium states) in the typical time scale of the process. This fact makes the fluid velocity $\mathbf{w}$ disappear from the diffusion-consumption equation for oxygen, which takes the form

$$D\Delta\sigma = \varphi(\sigma)\nu_V \,, \tag{27}$$

where D is the diffusion coefficient ($\simeq 2{\cdot}10^{-5}$ cm^2/sec) and oxygen consumption is represented by $\varphi(\sigma)$. According to experimental observations [13], $\varphi(\sigma)$ can be taken as a function of Michaelis-Menten type, which can be different in P and in Q, with a smooth interpolation in T. Moreover, $\varphi(\sigma_N) > 0$ has been assumed. Of course the right-hand side of (27) is equal to zero in N.

We observe that equations (21)-(23) (or (24)-(25)) are not sufficient to determine $\nu_V, \nu_N, \mathbf{u}, \mathbf{w}$, even if the field $\mathbf{u}$ is purely radial. However, from assumption *(vi)*, $\nu_V + \nu_N = \nu^\star$ is constant and thus, introducing the quantity

$$\nu(r,t) = \frac{\nu_V(r,t)}{\nu^\star} \,, \quad \nu \in [0,1] \,, \tag{28}$$

from Eqs. (21), (22) and (24) we obtain

$$\frac{1}{r}\frac{\partial}{\partial r}(ru) = \begin{cases} \chi(\sigma)\nu - \mu_N(1-\nu) & \text{in } P \cup T \cup Q \\ -\tilde{\mu}_N & \text{in } N\,. \end{cases} \tag{29}$$

Therefore, from (21) and (29) we have

$$\frac{\partial \nu}{\partial t} + u\frac{\partial \nu}{\partial r} + \nu\big[\mu(\sigma) + \mu_C(c,\sigma) + \mu_R(\sigma,t) - (\chi(\sigma)+\mu_N)(1-\nu)\big] = 0\,, \tag{30}$$

where $u(r,t)$ denotes $|\mathbf{u}|$. Using the boundary condition

$$u(r_0,t) = 0\,, \tag{31}$$

we get the following equation for the velocity field:

$$ru(r,t) = \int_{r_0}^{r} r'[(\chi(\sigma)+\mu_N)\nu - \mu_N]\,dr'\,, \quad r_0 < r \le \rho_N(t)\,. \tag{32}$$

Moreover, we can rewrite the equation (27) for σ in the form

$$\Delta\sigma = f(\sigma)\nu\,, \tag{33}$$

where $f(\sigma) = \varphi(\sigma)\nu^\star/D$, and the boundary condition

$$\sigma(r_0,t) = \sigma^\star \tag{34}$$

will be imposed to (33). We remark that the computation of the field $\mathbf{w}$ can be avoided owing to the assumption *(vi)*. The consequence of relaxing *(vi)* is to bring the full fluid dynamics in the model. Despite its great difficulty, the resulting problem is certainly worth to be investigated.

A crucial point is the determination of the cord/necrosis interface $r = \rho_N(t)$. Ordinarily (for instance in the equilibrium condition when $\mu_C = \mu_R = 0$) the necrotic region is continuously fed (as already seen in section 2), that is, the cells cross the interface $r = \rho_N(t)$. In this case, *i.e.*, when $u(\rho_N,t) > \dot{\rho}_N(t)$, the following free boundary conditions have to be imposed:

$$\sigma(\rho_N(t),t) = \sigma_N \tag{35}$$

$$\left.\frac{\partial \sigma}{\partial r}\right|_{r=\rho_N(t)} = 0\,. \tag{36}$$

By contrast, there are situations in which the interface $r = \rho_N(t)$ defined by Eqs. (35) and (36) tends to acquire a velocity larger than $u(\rho_N,t)$. This happens when a sudden massive destruction of cells rapidly lowers oxygen consumption. Clearly, a sign inversion of the difference $u(\rho_N,t)$–$\dot{\rho}_N$ is not allowed, because the necrotic material cannot be converted to living cells, and thus the following constraint must be satisfied

$$u(\rho_N(t),t) \ge \dot{\rho}_N\,. \tag{37}$$

When, solving the unconstrained problem, the inequality (37) is violated, we must change the free boundary conditions and let the interface ρ_N become a *material* surface, moving with the same velocity of the cells. So, Eq. (35) is replaced by

$$\dot{\rho}_N = u(\rho_N,t)\,, \tag{38}$$

while (36) is still valid.

Also the new free boundary problem is subjected to a constraint. Indeed, the switch from (35), (36) to (38), (36) will make $\sigma(\rho_N(t),t)$ raise above σ_N. However $\sigma(\rho_N(t),t)$ may later decrease and tend to drop below σ_N. In view of assumption *(iii)* this event is also forbidden, and in fact it marks the necessity of returning to the previous free boundary conditions. So, while (35), (36) must respect the constraint (37), the alternative formulation (38), (36) has to satisfy the constraint

$$\sigma(\rho_N(t),t) \geq \sigma_N\,. \tag{39}$$

The presence of constraints in the formulation of the model leads to a non-standard free boundary problem.

Concerning the motion of the outer boundary $B(t)$ of the necrotic region, since this boundary is a material surface, we write

$$\dot{B} = u(B,t)\,, \tag{40}$$

where $u(r,t)$ in the necrotic region can be easily expressed taking into account Eq. (29), obtaining

$$ru(r,t) = \rho_N(t)u(\rho_N(t),t) - (\tilde{\mu}_N/2)(r^2-\rho_N^2(t))\,, \quad r>\rho_N(t)\,. \tag{41}$$

Equation (40) requires an initial condition

$$B(0) = B_0\,, \tag{42}$$

and the same is true for the equation for $\nu(r,t)$, *i.e.*, equation (30),

$$\nu(r,0) = \nu_0(r)\,. \tag{43}$$

On the contrary, $\nu(r_0,t)$ has not to be prescribed, because $r=r_0$ is a characteristic curve for (30), owing to (31). According to the elliptic nature of the equation for σ, we are not allowed to prescribe $\sigma(r,0)$, but there must be some compatibility among ν, σ and B at $t=0$. The most natural choice is to let the system evolve from the stationary solution corresponding to $\mu_C=\mu_R=0$. We will discuss the statement of the steady-state problem in the next section.

The concentration of the cytotoxic chemical, appearing in Eq. (30), evolves according to a transport equation. Assuming that diffusion is the prevailing mechanism, we obtain the following diffusion-reaction equation

$$\frac{\partial c}{\partial t} - D_C\Delta c = -\varphi_C(c,\sigma)\nu^\star\nu - \lambda c\,, \tag{44}$$

with

$$c(r_0,t) = c^\star(t)\,, \tag{45}$$

$$\left.\frac{\partial c}{\partial r}\right|_{r=B(t)} = 0\,, \tag{46}$$

$$c(r,0) = 0\,. \tag{47}$$

In Eq. (44), D_C is the diffusion coefficient of the drug, $\varphi_C(c,\sigma)$ represents the net rate of drug uptake and metabolism by the tumour cells, and λ represents a possible additional loss not related to tumour cells. The function $c^\star$ in (45) represents the pharmacokinetics of the drug in the tumour vasculature. The function $\varphi_C(c,\sigma)$ is assumed continuously differentiable, increasing in c and vanishing for $c=0$, and the function $c^\star(t)$ to be nonnegative, continuously differentiable and vanishing for $t=0$.

4. The untreated cord

4.1. Properties of the stationary solution

Depending on the values of the model parameters, two cases are possible for the stationary state (with $\mu_C = \mu_R = 0$) of the model described in section 3: the necrotic region can be present (Case I) or not (Case II).

The stationary problem in Case I consists in determining the functions $\sigma(r)$, $\nu(r)$, $u(r)$, with $\nu \in [0,1]$, and two constants B and ρ_N, $B > \rho_N$, that satisfy

$$\Delta\sigma = f(\sigma)\nu\,, \quad r_0 < r < \rho_N\,, \tag{48}$$

$$\sigma(r_0) = \sigma^\star\,, \tag{49}$$

$$\sigma(\rho_N) = \sigma_N\,, \tag{50}$$

$$\left.\frac{d\sigma}{dr}\right|_{r=\rho_N} = 0\,, \tag{51}$$

$$\frac{d\nu}{dr} = -\frac{1}{u}[\mu(\sigma) - (\chi(\sigma) + \mu_N)(1-\nu)]\nu\,, \quad r_0 < r < \rho_N\,, \tag{52}$$

$$ru(r) = \begin{cases} \int_{r_0}^{r} r'[(\chi(\sigma) + \mu_N)\nu - \mu_N]\,dr'\,, & r_0 < r \le \rho_N \\ \rho_N u(\rho_N) - (\tilde{\mu}_N/2)(r^2 - \rho_N^2)\,, & \rho_N < r \le B\,, \end{cases} \tag{53}$$

$$u(B) = 0\,. \tag{54}$$

In Case II we drop the unknown ρ_N, and the boundary $r = B$ will limit a region filled only by tumour tissue. Now Eqs. (48), (52) and the first in (53) must be satisfied for $r_0 < r < B$. Equations (49) and (54) are preserved, while (50) and (51) change to

$$\sigma(r) > \sigma_N\,, \quad \text{for } r_0 < r < B\,, \quad \sigma(B) \ge \sigma_N \tag{50'}$$

$$\left.\frac{d\sigma}{dr}\right|_{r=B} = 0\,. \tag{51'}$$

Case II is expected to occur when μ and μ_N are sufficiently large, so that a substantial volume of dead cells is removed so quickly that u vanishes before σ reaches the threshold σ_N. Numerical calculations confirmed this conjecture. In [6] it is proved the following:

Theorem 4.1. *Under the assumptions previously stated, the steady state problem has one and only one solution, either exhibiting Case I or Case II.*

We give here only a sketch of the basic idea of the proof. A "shooting" parameter $\Sigma^\star$ has been introduced, together with the corresponding family of auxiliary problems in which the Cauchy data are prescribed for Eq. (48), namely (51) and

$$\left.\frac{d\sigma}{dr}\right|_{r=r_0} = \Sigma^\star < 0\,, \tag{55}$$

disregarding for the moment the free boundary conditions. These solutions are put in three different classes, according to which of the quantities $\sigma_r, \sigma - \sigma_N, u$ vanishes first. We denote

these classes by α, β, γ respectively. The monotone dependence of the solutions upon $\Sigma^\star$ allows to identify the solution of the original problem as the only separatrix between the sets β, α (Case I) or γ, α (Case II).

We note that Eq. (52) is degenerate at r_0 because $u(r_0)=0$. Since we have assumed that for $\sigma \geq \sigma_P$ both the proliferation and death rates are constant, it is easy to see that the solution ν is constant and equal to

$$\nu_{max} = 1 - \frac{\mu_0}{\chi_0 + \mu_N} \tag{56}$$

for $r_0 < r < \rho_P$, ρ_P being the radius such that $\sigma(\rho_P)=\sigma_P$. Taking into account Eq. (56), it can be found that the condition $\chi_0 > \mu_0$ is necessary in order to have a positive velocity field. It is easy to check indeed that $\chi_0 - \mu_0$ is the value of the right derivative of u at r_0. Moreover, it can be proved [6] that the volume fraction ν remains positive and decreasing in the interval $(\rho_P, \rho_N]$, unless $\mu \equiv 0$, in which case $\nu(r)=1$ in $(r_0, \rho_N]$.

4.2. Assessment of model parameters from the hepatoma 3924A data

A rather complete experimental investigation of tumour cords at the stationary state was given by Moore *et al.* [28] for the hepatoma 3924A implanted in rats. In that paper, besides the mean cord and vessel radii, the values of the labelling index (LI, the fraction of the number of cells that are in S phase), of the mitotic index (MI, fraction of cells in mitosis) and of the necrotic index (NI, fraction of dead cells) at increasing distances from the central vessel, are reported. In [3], using the LI data and the durations of cell cycle phases given in [28], an estimation of the function $\theta(r)$ of model (7)-(9) was obtained. Here we will exploit together all these data, to assess the values of some parameters of the model in section 3 and the form of the functions $\chi(\sigma)$ and $\mu(\sigma)$.

The consideration of a population model structured in terms of a variable related to cell cycle, is required to relate the mitotic index to the proliferation rate χ. Let us suppose that the cell population is described by the model of Eqs. (1)-(3), neglecting for the moment the presence of dead cells since the NI data show that, in the tumour cords studied, dead cells are in a very small percentage. Equation (18) can be rewritten, using (17), as

$$\frac{1}{r}\frac{d}{dr}\left(ru\nu_C\right) = \bar{\chi}(r)\nu_C(r)\,, \tag{57}$$

where

$$\bar{\chi}(r) = \frac{\int_0^{T_c} (dv/da) n(a,r)\, da}{\int_0^{T_c} v(a) n(a,r)\, da + v(0) n_Q(r)} \tag{58}$$

is the proliferation rate at the radial distance r. Assuming $v(a) = v_0 + (v_0/T_c)a$, Eq. (58) becomes

$$\bar{\chi}(r) = \frac{1}{T_c}\, \frac{n_P(r)}{n_P(r) + n_Q(r) + (1/T_c)\int_0^{T_c} a n(a,r)\, da}\,. \tag{59}$$

Taking into account the boundary condition (2), the age density $n(a,r)$ can be approximated by a linear profile with value $2\theta(r) n(T_c, r)$ at $a=0$, and $n(T_c, r)$ at $a=T_c$. Moreover, since the duration T_M of the mitotic phase is very short compared to T_c, for the mitotic index we can write

$$MI(r) \simeq \frac{T_M\, n(T_c, r)}{n_P(r) + n_Q(r)}\,. \tag{60}$$

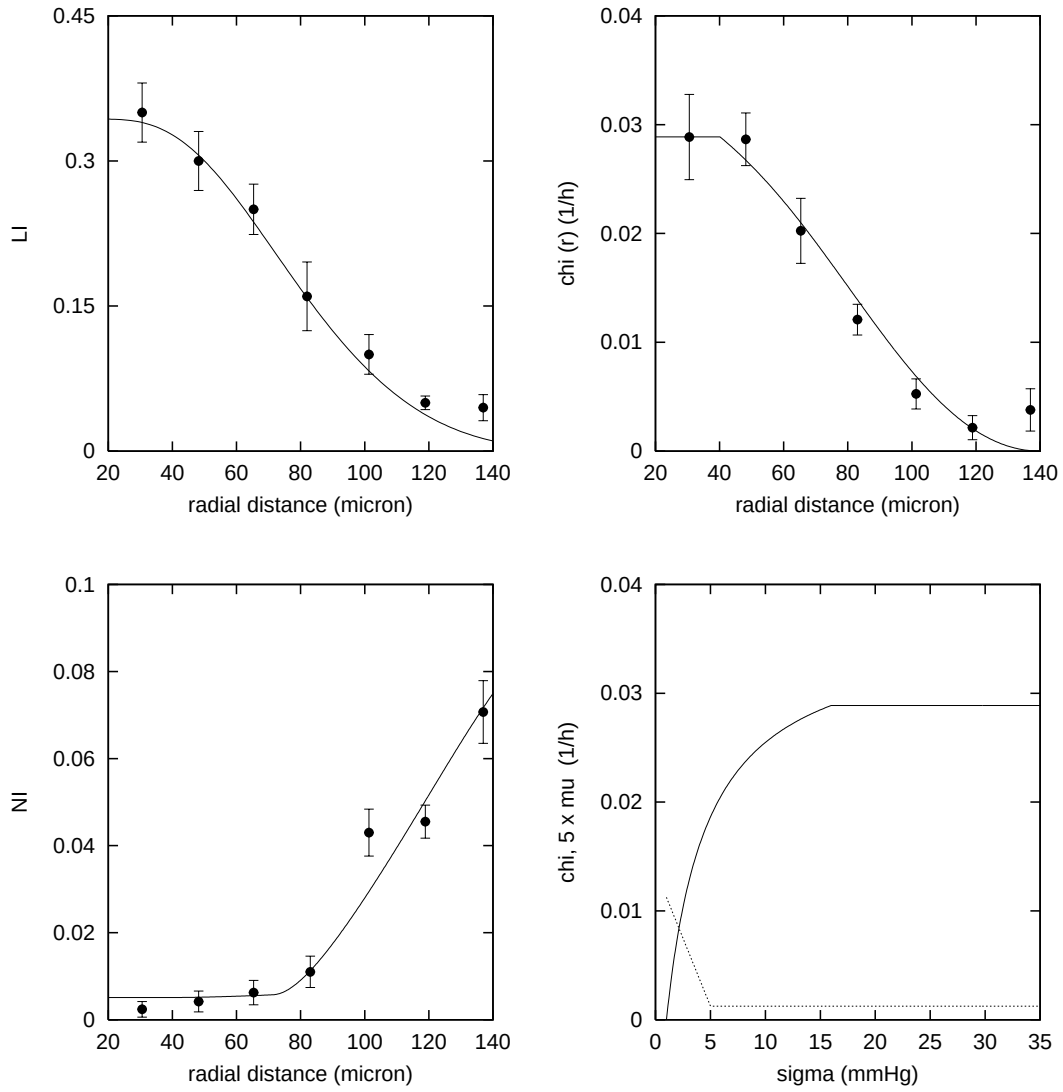

Fig. 2. Experimental data of LI (upper left panel) and NI (lower left) replotted from Moore *et al.* [28]. Data of $\bar{\chi}(r)$ (upper right) reconstructed by Eq. (61) using the MI data reported in [28]. Curves predicted by the model (solid lines). Estimated profiles of $\chi(\sigma)$ (solid line) and $\mu(\sigma)$ (dotted line) in the lower right panel. Parameter values (O_2 concentration in mmHg, length in μm, time in h): $r_0 = 20$, $\sigma^\star = 37$, $\sigma_P = 16$, $\sigma_Q = \sigma_N = 1$, $\mu_0 = 0.25 \cdot 10^{-3}$, $\mu_1 = 2.25 \cdot 10^{-3}$, $\sigma_\mu = 5$, $\mu_N = 0.02$. Moreover: $F_P = 0.016$, $F_Q = F_P/3$, $K_\sigma = 4.32$ [13].

Using these approximations in Eq. (59), leads to the following expression for $\bar{\chi}(r)$:

$$\bar{\chi}(r) \simeq \frac{\dfrac{1+2\theta(r)}{2}\,\dfrac{MI(r)}{T_M}}{1 + T_c \dfrac{1+\theta(r)}{3}\,\dfrac{MI(r)}{T_M}} \,. \tag{61}$$

The function $\chi(\sigma)$ can thus be searched in such a way that $\chi(\sigma(r))$ gives a good approximation of $\bar{\chi}(r)$.

Reconsidering the LI and MI data in [28], and assuming $T_S = 9.3\,\mathrm{h}$ and $T_{G2} = 3.7\,\mathrm{h}$ (the transit times in the phases S and $G2$ of the cell cycle reported in [28]), we obtained an improved fitting (see the LI in Fig. 2) with $T_c = 24\,\mathrm{h}$ (instead of 27.4 h as given in [28]), $T_M = 0.6\,\mathrm{h}$, and $\theta(r) = 1/(1+9[(r-r_0)/(\rho_N - r_0)]^{2.5})$. The theoretical curves, $LI(r)$ and $MI(r)$ were computed as

$$LI(r) = \int_{T_{G1}}^{T_{G1}+T_S} \phi(a,r)\,da\,, \qquad MI(r) = \int_{T_c-T_M}^{T_c} \phi(a,r)\,da\,, \tag{62}$$

where $T_{G1} = T_c - T_S - T_{G2} - T_M$ is the transit time in the $G1$ phase and $\phi(a,r)$ is the solution of Eqs. (7)-(9). Using these estimates of T_c, T_M and $\theta(r)$, the experimental values of MI have provided the values of $\bar{\chi}(r)$ reconstructed by Eq. (61) and reported in Fig. 2 (upper right panel). Further, as in [3], the consumption of oxygen was assumed to be described by

$$f(\sigma) = F(\sigma)\frac{\sigma}{K_\sigma + \sigma}\,, \qquad F(\sigma) = \begin{cases} F_P & \sigma \in [\sigma_P, \sigma^\star] \\ F_Q \dfrac{\sigma_P - \sigma}{\sigma_P - \sigma_Q} + F_P \dfrac{\sigma - \sigma_Q}{\sigma_P - \sigma_Q} & \sigma \in [\sigma_Q, \sigma_P] \\ F_Q & \sigma \in [\sigma_N, \sigma_Q] \end{cases} \tag{63}$$

with the values of the parameters F_P, F_Q and K_σ derived from [13] and indicated in the legend of Fig. 2. The threshold σ_N was fixed at 1 mmHg [18] and r_0 to 20 μm according to the values measured in the 3924A tumour cords.

Having thus fixed some of the model parameters, we tried to fit (by trial-and-error) the $\bar{\chi}$ data by the function $\chi(\sigma(r))$ and the NI data by $1-\nu(r)$, and to predict the cord radius. A reasonable fitting was obtained with $\chi(\sigma)$ and $\mu(\sigma)$ of the form shown in Fig. 2 (lower right panel), that is:

$$\chi(\sigma) = \begin{cases} \dfrac{\ln 2}{T_c}\,\dfrac{5(\sigma - \sigma_Q)/4}{\sigma - \sigma_Q + (\sigma_P - \sigma_Q)/4}, & \sigma_Q \le \sigma \le \sigma_P \\ \dfrac{\ln 2}{T_c}, & \sigma_P \le \sigma \end{cases} \tag{64}$$

$$\mu(\sigma) = \begin{cases} \mu_1 - (\mu_1 - \mu_0)\dfrac{\sigma - \sigma_N}{\sigma_\mu - \sigma_N}, & \sigma_N \le \sigma \le \sigma_\mu \\ \mu_0, & \sigma_\mu \le \sigma\,, \end{cases} \tag{65}$$

and with the values of $\sigma^\star$, σ_P, σ_Q, σ_μ, μ_0, μ_1 and μ_N reported in the legend of Fig. 2. In using the function $1-\nu(r)$ to fit the NI data, the mean volume of dead cells was implicitly assumed equal to the mean volume of viable cells, which is a good approximation in the case of uniform cell death. The above set of parameters gave ρ_N equal to 140.06 μm, which is very close to the mean cord radius experimentally observed (141 μm).

It has to be noted, however, that the same steady-state triple $(\nu(r), \sigma(r), \rho_N)$ can be achieved with an assigned $\chi(\sigma)$ and different pairs $(\mu(\sigma), \mu_N)$. This fact is easily recognized in the limit case of $\chi(\sigma)$ and $\mu(\sigma)$ constant. In this case, recalling Eq. (56), we can see that the same (constant) ν can be achieved at the steady state by two pairs (μ, μ_N) and (μ', μ'_N) such that

$$\frac{\mu'}{\chi + \mu'_N} = \frac{\mu}{\chi + \mu_N}\,,$$

provided that $\mu, \mu' < \chi$. Thus, the pair $(\mu(\sigma), \mu_N)$ cannot be uniquely identified on the basis of $\bar{\chi}$ and NI data, that give independent information on χ and ν, and the value given to μ_N was an *a priori* choice.

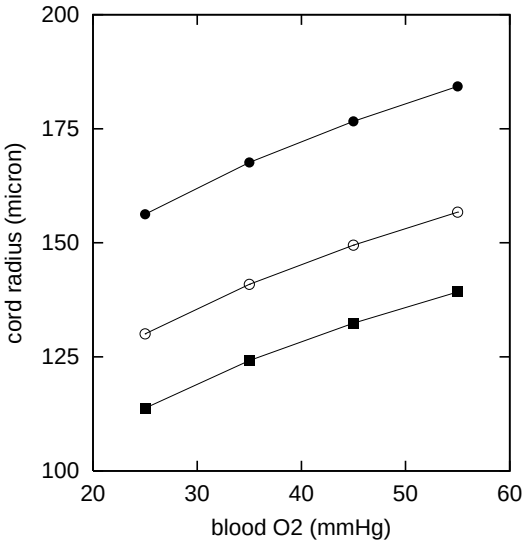

Fig. 3. Influence of $\sigma^\star$ on the stationary cord radius ρ_{N0}, for $r_0 = 10\,\mu$m (squares), $r_0 = 20\,\mu$m (white circles) and $r_0 = 40\,\mu$m (black circles).

To conclude this section, we show how the predicted cord radius changes when the vessel radius and the oxygen concentration in blood are changed, keeping the other parameters at the values previously found. In Fig. 3 we have reported ρ_N computed at increasing $\sigma^\star$ values within the physiological range, for three different r_0 values. It can be noted that, although $\sigma^\star$ is more than doubled, the stationary cord radius exhibits a markedly reduced variability.

5. The evolution problem and the behaviour of the solutions

5.1. The evolution problem

To describe the response of the cord, supposed at the stationary state, to a cell killing agent delivered at time $t = 0$, we have to consider the evolution in time of the model described in section 3. The evolution problem that arises was studied in [6], where the following theorem was proved:

Theorem 5.1. *Under the assumptions stated in section 3, a solution of the evolution problem exists globally in time.*

The solution was obtained as the limit of an approximating sequence constructed step by step through the procedure outlined in the following. The index 0 denotes the initial values. Fix a time T and divide it into n equal parts. In the first time step, first compute the integral curves of

$$\dot{\eta} = u_0(\eta)\,, \quad \eta(\hat{r}, 0) = \hat{r}\,, \qquad \hat{r} \in [r_0, B_0]\,. \tag{66}$$

As a consequence $B(t) \equiv B_0$.

Next solve the problem for c in $[r_0, B_0]\times[0, \theta], \theta = T/n$, setting $\varphi_C = 0$. With this determination of c integrate

$$D_u\nu = -\nu\left[\mu(\sigma_0) + \mu_R(\sigma_0, t) + \mu_C(c, \sigma_0) - (\chi(\sigma_0) + \mu_N)(1 - \bar{\nu}^0)\right] \equiv -\nu H(t, c, \sigma_0, \bar{\nu}^0) \tag{67}$$

where $\bar{\nu}^0$ is ν_0 evaluated at the point $(\xi(r,t), 0)$ connected to (r,t) by one of the curves (66), and D_u denotes differentiation along such a line. Knowing ν, we can solve the free boundary problem

for σ with Cauchy data $\sigma(\tilde{\rho}_N, t) = \sigma_N$ and $\sigma_r(\tilde{\rho}_N, t) = 0$, determining σ and the approximated interface $\tilde{\rho}_N(t)$. Then $\dot{\tilde{\rho}}_N$ must be compared with $u_0(\tilde{\rho}_N(t))$. If the comparison is satisfactory, we set $\rho_N = \tilde{\rho}_N$. With the knowledge of σ and ν the new velocity field can be computed for $t \in [0, \theta]$ using Eqs. (32) and (41). Then proceed to the second time step, replacing Eq. (66) with

$$\dot{\eta}(t) = u(\eta(t), t - \theta), \quad t \in (\theta, 2\theta)\,, \tag{68}$$

continuing the previous curves. The continuation of $B(t)$ is found similarly.

We go through the same points of the first step with the following linearizations: (i) in the problem for c, instead of $\varphi_C(c, \sigma)\nu$ we use $\varphi_C(c^\theta, \sigma^\theta)\bar{\nu}^\theta$, where $c^\theta = c(r, t-\theta)$, $\sigma^\theta = \sigma(r, t-\theta)$, and $\bar{\nu}^\theta$ is evaluated at the time $t = \theta$ on the line (68) crossing the point (r, t); (ii) the r.h.s. of (67) is replaced by $-\nu H(t, c, \sigma^\theta, \bar{\nu}^\theta)$. Once the problem for the pair $(\tilde{\rho}_N, \sigma)$ has been solved using the information already available, $\dot{\tilde{\rho}}_N$ must be compared with $u(\tilde{\rho}_N(t), t-\theta)$. If the comparison is satisfactory, we proceed to updating the velocity field $u(r, t)$, $t \in [\theta, 2\theta]$.

The procedure is carried out as described if the constraint (37) on the velocity is never violated. If the constraint is violated, one has to introduce the necessary changes to switch to the new free boundary conditions (36) and (38) on ρ_N. However, it is not guaranteed that we can always proceed for a finite interval before another switch be necessary. In other words, if the switches have an accumulation point, the construction of the approximated solution comes to a stop. This difficulty is overcome by introducing, for each n, a tolerance for the constraints which tends to zero as $n \to \infty$.

The convergence of this procedure was proved in [6] showing that the approximating sequence is compact with respect to a suitable norm. The uniqueness of the solution was also proved, but an additional assumption that limits the norm of the derivative of $f(\sigma)$ was needed.

5.2. The cord response to a single-dose treatment

The numerical solution of the evolutive problem has been obtained by a scheme that substantially implements the construction of the approximate solutions seen above. In [7], the cord response to a single-dose cell killing agent was investigated by simulations. Particular attention was given to the influence of oxygen concentration in modulating the treatment-induced cell death, by exploring also some extensions of the model formulation given in section 3.

We present here a simplified case, that however provides a prototype of the cord response, in which the rate of cell death induced by treatment is a function, $\beta(t)$, of time only. In this way we neglect the dependence of cell death on oxygen concentration that is observed in radiotherapy, and the possible changes of the cell death rate with the radial distance that, in the case of chemotherapy, are due to the transport of the drug. To describe the delayed effects that follow the delivery of a single dose of radiation or drug at $t = 0$, $\beta(t)$ will have the form of a broadened pulse. Although the delivery time can be very short (as in radiotherapy or when the drug is administered as a bolus and its pharmacokinetics is fast), cell death may continue indeed for many hours after delivery, sometimes even during the lifespan of the successive cell generations [11,25]. In the simulations that follow, as a basic pattern of $\beta(t)$, we assumed a trapezoidal shape of 12 h length, with a rising front lasting 2 h, a plateau of 8 h, and a descending front lasting 2 h. β_{max} will denote the plateau value. The other parameters of the simulation are indicated in the legend of Fig. 4.

Figure 4 shows the response of the cord. As indicated by the time evolution of $\sigma(\rho_N(t), t)$ (lower left panel), the cord boundary ρ_N, which is non-material at the stationary state (and in a right neighborhood of $t = 0$, since $\beta(t)$ grows continuously from zero), quickly turns into

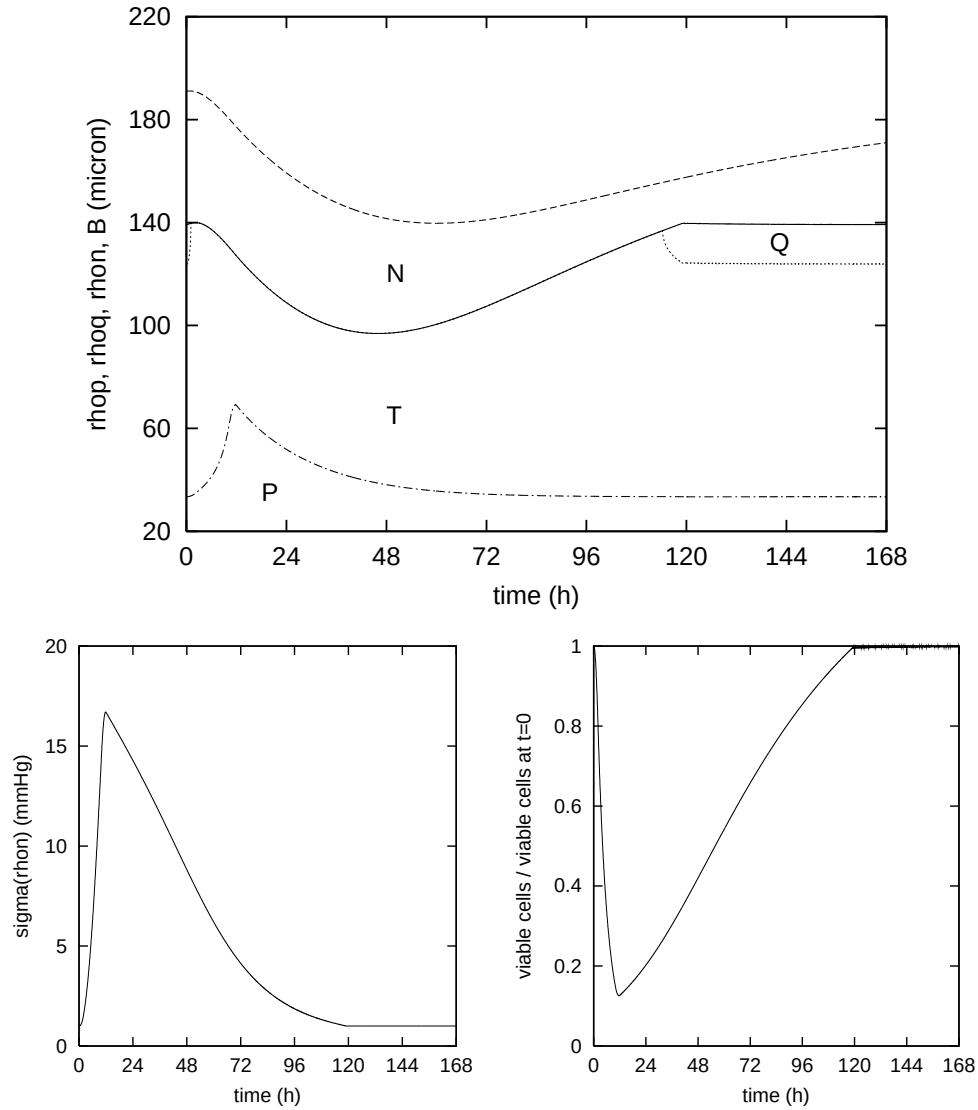

Fig. 4. Response of the tumour cord to a single-dose treatment. Geometrical variables (upper panel): ρ_N, solid line; B, dashed; ρ_Q, dotted; ρ_P, dash-dotted; the cord regions P, T, Q and N are also indicated. Oxygen concentration at the cord boundary (lower left panel) and normalized total fraction of viable cells (lower right panel). Parameter values (O_2 concentration in mmHg, length in μm, time in h): $r_0 = 20$, $\sigma^\star = 35$, $\sigma_P = 20$, $\sigma_Q = 1.125$, $\sigma_N = 1$, $\mu_N = 0.04$, $\tilde{\mu}_N = 0.01$. Moreover, F_P, F_Q and K_σ as in Fig. 2; $\chi(\sigma)$ increasing as a Michaelis-Menten curve in (σ_Q, σ_P) from 0 to $\chi_0 = \ln 2/T_c$, with $T_c = 24$, $\mu(\sigma) = 0$. Parameters of the treatment: $\beta_{max} = 0.24\,\mathrm{h}^{-1}$.

a material interface and so it remains during all the regression phase. Then, the boundary switches again to be non-material at some stage of the regrowth phase, when the necrotic region is once again entered by new cells (this point is marked by a slope discontinuity in $\rho_N(t)$). The simulations point out that not only the constraints (37) and (39) come into play, but that they actually have a crucial role. The figure also shows the time course of B, and of the radii ρ_P and ρ_Q where the oxygen tension has the values σ_P and σ_Q respectively. We recall that in the region P between r_0 and ρ_P the proliferation rate is maximal, whereas between ρ_Q and ρ_N (region Q) all cells are quiescent, with a transition region T in between. The time course of ρ_P

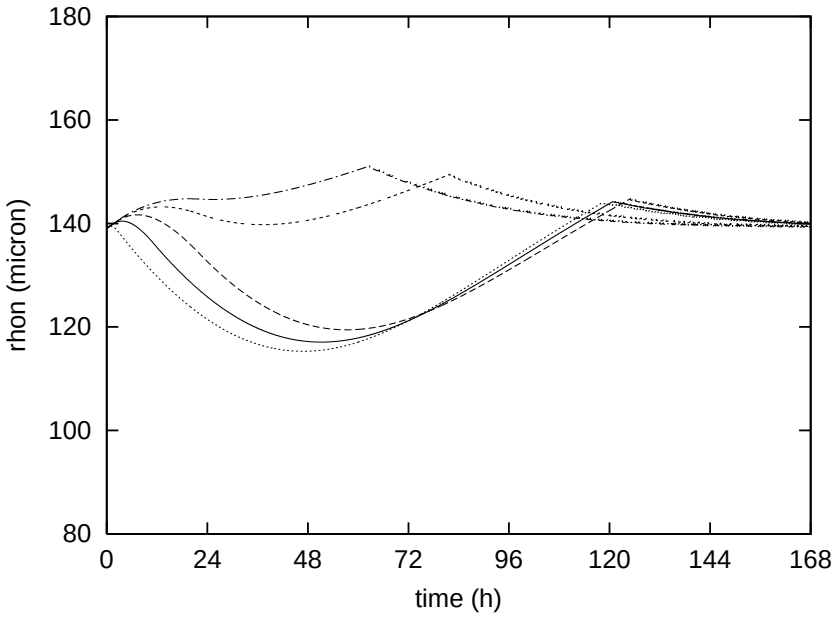

Fig. 5. Effect on the cord radius of different $\beta(t)$ patterns. Patterns with the same area: $k=4$ (dotted), $k=1$ (solid), $k=0.5$ (dashed). Patterns with reduced area: total length 24 h, $\beta_{max}=0.06\,\mathrm{h}^{-1}$ (small-dashed), $\beta_{max}=0.04\,\mathrm{h}^{-1}$ (dash-dotted). Other parameters as in Fig. 4, except $\mu_N=0.02\,\mathrm{h}^{-1}$.

and ρ_Q, together with that of $\sigma(\rho_N)$ in the lower left panel, reveals a substantial reoxygenation of the cord for a long period after the treatment. The lower right panel of Fig. 4 represents the ratio between the total volume (per unit cord length) of viable cells and its value at $t=0$, that is $\int_{r_0}^{\rho_N(t)} r\nu(r,t)\,dr / \int_{r_0}^{\rho_{N0}} r\nu(r,0)\,dr$, and shows the marked depletion of viable cells at the end of the time interval in which $\beta>0$. Whereas the minimum of viable cell number occurs at that time, the minima of ρ_N and B occur later, this fact being related to the non-instantaneous degradation of dead cells. The predicted cord response, showing a regression followed by a regrowth, is in qualitative agreement with the experimental data reported in [32,26,27,16].

Figure 5 shows the effects of treatments with different $\beta(t)$ patterns. First, we have considered patterns with the same area and increasing sharpness, assuming $\beta(t)=k\tilde{\beta}(kt)$ where $\tilde{\beta}(t)$ has the trapezoidal shape described above. When the death rate approaches an impulse, the cord response appears to converge to a limit behaviour. In response to low intensity treatments (with reduced areas), the cord shows, rather unexpectedly, a slight increment of its radius. A moderate cell death with a small reduction in ν, in fact, may be unable to produce the inversion of the velocity at $r=\rho_N$; on the other hand, the reduced oxygen consumption does allow cell viability at values of ρ_N larger than the stationary value. During this cord expansion, of course, the total volume of viable cells initially decreases and thus the density of viable cells in the cord is reduced.

5.3. The cord response to impulsive cell death

To gain insight into the model behaviour in describing the response to a single-dose treatment, and elucidate the role of the major parameters, we consider now the ideal case in which the rate of treatment-induced cell death is a Dirac delta function. In this case, μ_R and μ_C are set to zero in Eq. (30) and the effect of treatment is embodied in the new initial condition

$$\nu(r, 0^+) = \alpha(\sigma_0(r))\nu_0(r)\,, \tag{69}$$

where α is dependent in general on the oxygen concentration and it is $\alpha(\sigma) \leq 1$. Since Eqs. (33)-(36) cannot be satisfied with ν given by the initial condition (69) and $\rho_N = \rho_{N0}$, it can be recognized that $\rho_N(t)$ will be a material interface in a right neighborhood of $t=0$.

We consider the very simplified situation in which $\mu=0$ (so that $\nu_0(r)=1$, see Eq. (56)), $\chi(\sigma)$ is independent of σ and equal to χ, and $\alpha(\sigma)=\alpha<1$. The equation for ν becomes independent of σ and is written as

$$\frac{\partial \nu}{\partial t} + u\frac{\partial \nu}{\partial r} = (\chi + \mu_N)(1-\nu)\nu\,, \tag{70}$$

$$\nu(r, 0) = \alpha\,, \tag{71}$$

with u given by Eq. (32). It is easy to see that a solution of Eqs. (70)-(71) is $\nu(r,t)=y(t)$, $y(t)$ being the solution of the logistic equation

$$\dot{y} = (\chi + \mu_N)(1-y)y \tag{72}$$

$$y(0) = \alpha\,. \tag{73}$$

This solution is the unique solution of Eqs. (70)-(71). In fact, let us consider any possible solution, and consider its values along the characteristic lines of (70). Writing the derivative along the characteristic lines and taking into account that the initial condition is constant with r, we can see that at any given time the value of ν is the same on all the characteristic lines, and equal to $y(t)$. Having found ν, $u(r,t)$ can be written explicitly and, as long as the boundary $\rho_N(t)$ remains a material interface, $\rho_N(t)$ also can be written explicitly. Taking into account that Eqs. (32) and (38) give

$$\rho_N(t)\dot{\rho}_N(t) = \int_{r_0}^{\rho_N(t)} r'[(\chi+\mu_N)y(t) - \mu_N]\,dr' \tag{74}$$

and that

$$y(t) = \Big(\frac{1-\alpha}{\alpha}\mathrm{e}^{-(\chi+\mu_N)t} + 1\Big)^{-1}\,, \tag{75}$$

we obtain

$$\frac{\rho_N^2(t) - r_0^2}{\rho_{N0}^2 - r_0^2} = \alpha\mathrm{e}^{\chi t} + (1-\alpha)\mathrm{e}^{-\mu_N t}\,. \tag{76}$$

The above equation shows that the cord can initially shrink or expand according to the value of α. In fact, a critical value exists

$$\hat{\alpha} = \frac{\mu_N}{\chi + \mu_N}\,, \tag{77}$$

such that if $\alpha > \hat{\alpha}$ it is $\dot{\rho}_N(0^+) > 0$, whereas if $\alpha < \hat{\alpha}$ it is $\dot{\rho}_N(0^+) < 0$. When $\alpha < \hat{\alpha}$, $\rho_N(t)$ will attain a minimum at

$$t_{min} = \frac{1}{\chi + \mu_N}\,\ln\Big(\frac{1-\alpha}{\alpha}\,\frac{\mu_N}{\chi}\Big)\,, \tag{78}$$

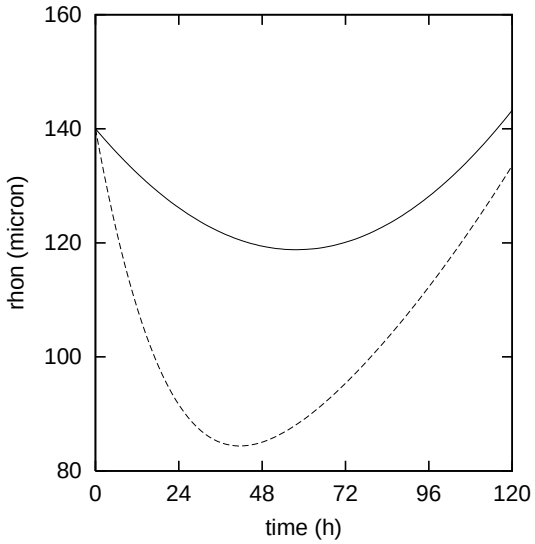

Fig. 6. Plot of $\rho_N(t)$ as given by Eq. (76); $\alpha = 0.15$, $\chi = 0.015\,\mathrm{h}^{-1}$, $\mu_N = 0.015\,\mathrm{h}^{-1}$ (solid line) and $\mu_N = 0.06\,\mathrm{h}^{-1}$ (dashed line).

and then $\rho_N(t)$ will be increasing until $\sigma(\rho_N(t),t) = \sigma_N$. The oxygen concentration $\sigma(\rho_N(t),t)$, which is larger than σ_N at $t = 0^+$, will indeed be decreasing with time for $t > t_{min}$. To see this, we use the monotonicity property of σ with respect to ν and ρ_N, reported in the Appendix. Since $\partial\sigma/\partial\nu < 0$ (see $(A7)$), and at $t = 0^+$ ρ_N is not changed whereas ν is decreased, we have $\sigma(\rho_{N0}, 0^+) > \sigma_N$. For $t > 0$, taking into account the dependence of $\sigma(r,t)$ on $\nu(t)$ and $\rho_N(t)$, and that $\sigma_r(\rho_N(t),t) = 0$, we can write

$$\frac{d}{dt}\sigma(\rho_N(t),t) = \frac{\partial\sigma}{\partial\nu}\dot{\nu} + \frac{\partial\sigma}{\partial\rho_N}\dot{\rho}_N\,. \tag{79}$$

This quantity, also because $\partial\sigma/\partial\rho_N < 0$ (see $(A16)$), is negative when $\rho_N(t)$ is increasing. Moreover, the value σ_N will be reached at a finite time. In fact, let us suppose that $\sigma(r,t) > \sigma_N$, $r \in [r_0, \rho_N]$, for all $t > 0$. The value of σ at ρ_N can be written as

$$\sigma(\rho_N(t),t) = \sigma^\star - y(t)\int_{r_0}^{\rho_N(t)} r f(\sigma(r,t)) \log\frac{r}{r_0}\,dr\,. \tag{80}$$

Taking into account that $f(\sigma) > f(\sigma_N)$ if $\sigma > \sigma_N$, we obtain

$$\begin{aligned}\sigma(\rho_N(t),t) - \sigma^\star &< -y(t) f(\sigma_N)\int_{r_0}^{\rho_N(t)} r\log\frac{r}{r_0}\,dr \\ &= -y(t) f(\sigma_N)\left(\frac{\rho_N^2(t)}{2}\log\frac{\rho_N(t)}{r_0} - \frac{\rho_N^2(t)}{4} + \frac{r_0^2}{4}\right).\end{aligned} \tag{81}$$

Since, according to Eq. (76), $\rho_N(t)$ is increasing and unbounded for t large, Eq. (81) implies that $\sigma(\rho_N(t),t) \to -\infty$ as $t \to \infty$, that contradicts the hypothesis. Thus, there will exist a finite time $\bar{t}$ at which $\sigma(\rho_N(t),t)$ is equal to σ_N.

At the time $\bar{t}$ the cord radius is necessarily larger than ρ_{N0}, since $\nu(r,\bar{t}) = y(\bar{t}) < 1$, and the boundary switches to be non-material. Thereafter the boundary will tend monotonically to ρ_{N0} as $y(t) \to 1$. Figure 6 shows $\rho_N(t)$ as predicted by Eq. (76), for α and χ fixed and different values of μ_N. As expected, when μ_N is increased the shrinkage is more pronounced and, if μ_N is larger than χ, the shrinkage is faster than the regrowth of the cord.

In the general case in which χ depends on σ, χ_0 being its maximal value, we can see that the evolution of the cord radius, $\rho_N^0(t)$, given by Eq. (76) with $\chi = \chi_0$, dominates the actual $\rho_N(t)$ (until both these boundaries are material). Let us consider the quantities

$$X_V(t) = \int_{r_0}^{\rho_N(t)} r\nu_V(r,t)\, dr \tag{82}$$

$$X_N(t) = \int_{r_0}^{\rho_N(t)} r\nu_N(r,t)\, dr\,, \tag{83}$$

that is, the total volumes (divided by 2π, and per unit cord length) of viable cells and dead cells, respectively. By integrating from r_0 to ρ_N Eqs. (21)-(22) multiplied by r, as long as $\rho_N(t)$ is a material boundary we have

$$\dot{X}_V(t) = \int_{r_0}^{\rho_N(t)} r\chi(\sigma(r,t))\nu_V(r,t)\, dr \le \chi_0 X_V(t) \tag{84}$$

$$\dot{X}_N(t) = -\mu_N X_N(t)\,. \tag{85}$$

Moreover, taking into account Eq. (29), we get

$$\rho_N(t)\dot{\rho}_N(t) = \dot{X}_V(t) + \dot{X}_N(t)\,. \tag{86}$$

Denoting by $X_V^0(t)$ and $X_N^0(t)$ the volumes defined by Eqs. (82)-(83) in the case of $\chi(\sigma) = \chi_0$, it is easy to recognize that $X_V^0(t) \ge X_V(t)$ (because $\dot{X}_V^0 = \chi_0 X_V^0$ and the initial conditions are the same) and $X_N^0(t) = X_N(t)$. Thus it is

$$\rho_N\dot{\rho}_N \le \chi_0 X_V - \mu_N X_N \le \chi_0 X_V^0 - \mu_N X_N^0\,. \tag{87}$$

Since the last expression in (87) gives $\rho_N^0\dot{\rho}_N^0$, we obtain $\rho_N(t) \le \rho_N^0(t)$ for $t \ge 0$ and until both ρ_N and ρ_N^0 are material boundaries.

As an example of how the approximation (78) behaves, we have considered the response to the shortest $\beta(t)$ in Fig. 5 (dotted line), and compared the time of the minimum of the cord radius with the estimate given by Eq. (78). The value of α was set to the minimum of the relative volume of viable cells attained in the simulation ($\alpha = 0.097$), $\chi = \chi_0 = 0.029\,\mathrm{h}^{-1}$ and $\mu_N = 0.02\,\mathrm{h}^{-1}$. The estimate was $t_{min} = 37.9\,\mathrm{h}$, whereas the value in Fig. 5 was 46.9 h. As expected, because the actual χ is overestimated by χ_0, the approximated response is faster than the actual one, however the time of the maximal regression is estimated within a 20% error.

6. Concluding remarks

Developing mathematical models of proliferating cell populations with spatial structure and subjected to cell migration, involves the consideration of many different aspects, from the biology of cell cycle, to the mechanical interactions governing the cell motions, and to the transport of nutrients.

In this paper we have reviewed models of tumour cords in which the cell population is described with age or cell maturity structure, or the cells are simply viewed as a component of a mixture and the population is characterized in terms of the fraction of volume occupied locally by the cells. By means of this simpler approach, and by including in the model the oxygen and drug transport, a reasonable description of the response of tumour cords to single-dose treatments was achieved. A peculiar feature of this model is that the boundary between the cord and the necrotic region, during its evolution after the treatment, may switch from being a non-material interface (defined as the radius at which the oxygen concentration attains a critical value) to being a material one, and viceversa.

The consideration of models that include a representation of the cell cycle, besides allowing us the analysis of experimental data obtained by cell labelling with DNA precursors, appears on the other hand of importance for a better prediction of the effect of radiation and drugs. It is well known, in fact, that the action of most agents shows a marked cell-cycle phase specificity. In such a way, the complex pattern of cytostatic and cell-killing effects that characterize the cellular response to anticancer agents would be more completely addressed.

A critical assumption of the models here discussed is the invariance of the total cell number in the unit volume, or of the volume fraction occupied by the cells. This assumption leads, in the adopted geometry, to a purely kinematic approach for the determination of the cell velocity field. Although this assumption appears to be reasonable in the untreated cord on the basis of some experimental observations, it is likely that the fraction of extracellular fluid be subjected to changes during treatments inducing cell death. If this assumption is relaxed, the momentum balance must be considered both for the cells and the extracellular materials. This improvement in the modelling would provide a more realistic representation of the cord and tumour mass evolution and we plan to deal with this point in the future.

Appendix: Monotonicity properties of the oxygen concentration profile

Let us consider the following problem, that defines the oxygen concentration within the cord as a function of the radial distance:

$$\Delta\sigma = f(\sigma)\nu \tag{A1}$$

$$\sigma(r_0) = \sigma^\star \tag{A2}$$

$$\sigma_r(\rho_N) = 0\,, \tag{A3}$$

in the case in which ν is constant with r. The solution will be dependent on ν and ρ_N, *i.e.* $\sigma = \sigma(r, \nu, \rho_N)$.

We consider first the dependence of σ on ν (for fixed ρ_N). Let us denote $\omega(r) = \partial\sigma/\partial\nu$. By differentiating $(A1)$-$(A3)$ with respect to ν, we obtain

$$\omega_{rr} + \frac{1}{r}\omega_r = f'(\sigma(r))\omega(r)\nu + f(\sigma(r)) \tag{A4}$$

$$\omega(r_0) = 0 \tag{A5}$$

$$\omega_r(\rho_N) = 0\,. \tag{A6}$$

From $(A4)$, for every r where $\omega_r = 0$, it follows that

$$\omega_{rr} < 0 \qquad \text{if } \omega < -\frac{f(\sigma)}{f'(\sigma)\nu}$$

$$\omega_{rr} > 0 \qquad \text{if } \omega > -\frac{f(\sigma)}{f'(\sigma)\nu}\,,$$

with $-f(\sigma)/(f'(\sigma)\nu) < 0$ and increasing with r. Thus $\omega(r)$, for $r > r_0$, can only be negative with a minimum larger than $\inf[-f(\sigma)/(f'(\sigma)\nu)]$. Therefore

$$-\frac{f(\sigma^\star)}{f'(\sigma^\star)\nu} < \frac{\partial\sigma}{\partial\nu} < 0\,, \quad r_0 < r \le \rho_N\,. \tag{A7}$$

Concerning now the dependence of σ on ρ_N (for fixed ν), let us consider the Cauchy problem defined by Eqs. $(A1)$-$(A2)$ and by

$$\sigma_r(r_0) = \Sigma^\star\,, \tag{A8}$$

with $\Sigma^\star$ such that the solution has a positive minimum. We can write

$$r\sigma_r(r) = r_0\Sigma^\star + \nu\int_{r_0}^{r} r' f(\sigma(r'))\,dr' \tag{A9}$$

and

$$\sigma(r) = \sigma^\star + r_0\Sigma^\star \log\frac{r}{r_0} + \nu\int_{r_0}^{r} r' f(\sigma(r'))\log\frac{r'}{r_0}\,dr'\,. \tag{A10}$$

Differentiating $(A10)$ with respect to $\Sigma^\star$, we obtain the following linear integral equation in $\partial\sigma/\partial\Sigma^\star$

$$\frac{\partial\sigma}{\partial\Sigma^\star} = r_0\log\frac{r}{r_0} + \nu\int_{r_0}^{r} r' f'(\sigma(r'))\frac{\partial\sigma}{\partial\Sigma^\star}\log\frac{r'}{r_0}\,dr'\,, \tag{A11}$$

so that, for $r > r_0$,

$$\frac{\partial\sigma}{\partial\Sigma^\star} > 0\,. \tag{A12}$$

Differentiating $(A9)$ with respect to $\Sigma^\star$ we have

$$r\frac{\partial\sigma_r}{\partial\Sigma^\star} = r_0 + \nu\int_{r_0}^{r} r' f'(\sigma(r'))\frac{\partial\sigma}{\partial\Sigma^\star}\,dr'\,, \tag{A13}$$

that implies, in view of $(A12)$,

$$\frac{\partial\sigma_r}{\partial\Sigma^\star} > 0\,. \tag{A14}$$

Therefore, as $\Sigma^\star$ increases, the radius $\rho_N = \rho_N(\Sigma^\star)$ where $\sigma_r = 0$ will decrease, so that $\partial\rho_N/\partial\Sigma^\star < 0$. Considering now the original problem $(A1)$-$(A3)$, we can define the function $\Sigma^\star(\rho_N)$, which

gives the value of $\sigma_r(r_0)$ as a function of ρ_N. Since this function is the inverse of the function $\rho_N(\Sigma^\star)$ defined by the problem $(A1)$, $(A2)$ and $(A8)$, we have

$$\frac{\partial \Sigma^\star}{\partial \rho_N} < 0\,. \tag{A15}$$

Thus, in view of the inequalities $(A12)$, $(A14)$ and $(A15)$, it follows

$$\frac{\partial \sigma}{\partial \rho_N} < 0\,, \quad r_0 < r \leq \rho_N \tag{A16}$$

$$\frac{\partial \sigma_r}{\partial \rho_N} < 0\,, \quad r_0 \leq r < \rho_N\,. \tag{A17}$$

References

1. J.A. Adam and S.A. Maggelakis (1990) Diffusion regulated growth characteristics of a spherical prevascular carcinoma. *Bull. Math. Biol.* **52**, 549-582.

2. D. Ambrosi and L. Preziosi (2002) On the closure of mass balance models for tumour growth. *Math. Models Methods Appl. Sci.* **12**, 737-754.

3. A. Bertuzzi and A. Gandolfi (2000) Cell kinetics in a tumour cord. *J. theor. Biol.* **204**, 587-599.

4. A. Bertuzzi, A. Fasano and A. Gandolfi (2000) A mathematical model for the growth of tumor cords incorporating the dynamics of a nutrient. In *Free Boundary Problems: Theory and Applications II* (N. Kenmochi, Ed.), Math. Sci. Appl. 14, Gakkotosho, Tokyo, pp. 31-46.

5. A. Bertuzzi, A. Fasano, A. Gandolfi and D. Marangi (2002) Cell kinetics in tumour cords studied by a model with variable cell cycle length. *Math. Biosci.* **177-178**, 103-125.

6. A. Bertuzzi, A. Fasano and A. Gandolfi, A free boundary problem with unilateral constraints describing the evolution of a tumour cord under the influence of cell killing agents, submitted.

7. A. Bertuzzi, A. d'Onofrio, A. Fasano and A. Gandolfi, Regression and regrowth of tumour cords following single-dose anticancer treatment, submitted.

8. M.I.G. Bloor and M.J. Wilson (1997) A mathematical model of a micrometastasis. *J. Theor. Med.* **1**, 153-168.

9. M.I.G. Bloor and M.J. Wilson (1999) The non-uniform spatial development of a micrometastasis. *J. Theor. Med.* **2**, 55-71.

10. C.J.W. Breward, H.M. Byrne and C.E. Lewis (2002) The role of cell-cell interactions in a two-phase model for avascular tumour growth. *J. Math. Biol.* **45**, 125-152.

11. R.G. Bristow and R.P. Hill (1998) Molecular and cellular basis of radiotherapy. In *The Basic Science of Oncology* (eds. I.F. Tannock and R.P. Hill), New York: McGraw-Hill, pp. 295-321.

12. H.M. Byrne and M.A.J. Chaplain (1995) Growth of nonnecrotic tumors in the presence and absence of inhibitors. *Math. Biosci.* **130**, 151-181.

13. J.J. Casciari, S.V. Sotirchos and R.M. Sutherland (1992) Variations in tumor cell growth rates and metabolism with oxygen concentration, glucose concentration, and extracellular pH. *J. Cell. Physiol.* **151**, 386-394.

14. S. Cui and A. Friedman (2001) Analysis of a mathematical model of the growth of necrotic tumors. *J. Math. Anal. Appl.* **255**, 636-677.

15. J. Dyson, R. Villella-Bressan and G. Webb, The steady state of a maturity structured tumor cord cell population, in press.

16. K.H. Falkvoll (1990) The relationship between changes in tumour volume, tumour cell density and parenchimal cord radius in a human melanoma xenograft exposed to single dose irradiation. *Acta Oncol.* **29**, 935-939.

17. H.P. Greenspan (1972) Models for the growth of a solid tumor by diffusion. *Stud. Appl. Math.* **51**, 317-340.

18. K. Groebe and P. Vaupel (1988) Evaluation of oxygen diffusion distances in human breast cancer xenografts using tumor-specific in vivo data: role of various mechanisms in the development of tumor hypoxia, *J. Radiat. Oncol. Biol. Phys.* **15**, 691-697.

19. D.G. Hirst and J. Denekamp (1979) Tumour cell proliferation in relation to the vasculature. *Cell Tissue Kinet.* **12**, 31-42.

20. D.G. Hirst, V.K. Hirst, B. Joiner, V. Praise and K.M. Shaffi (1991) Changes in tumour morphology with alterations in oxygen availability: further evidence for oxygen as a limiting substrate. *Br. J. Cancer* **64**, 54-58.

21. J. Holash, P.C. Maisonpierre, D. Compton, P. Boland, C.R. Alexander, D. Zagzag, G.D. Yankopoulos and S.J. Wiegand (1999) Vessel cooption, regression, and growth in tumors mediated by angiopoietins and VEGF. *Science* **284**, 1994-1998.

22. L. Holmgren, M.S. O'Reilly and J. Folkman (1995) Dormancy of micrometastases: balanced proliferation and apoptosis in presence of angiogenesis suppression. *Nature Med.* **1**, 149-153.

23. S.R. Lubkin, and T. Jackson (2002) Multiphase mechanics of capsule formation in tumors. *J. Biomech. Eng.* **124**, 237-243.

24. D.L.S. McElwain and P.J. Ponzo (1977) A model for the growth of a solid tumor with non-uniform oxygen consumption. *Math. Biosci.* **35**, 267-279.

25. F. Montalenti, G. Sena, P. Cappella and P. Ubezio (1998) Simulating cancer cell kinetics after drug treatment: application to Cisplatin on ovarian carcinoma. *Phys. Rev. E* **57**, 5877-5887.

26. J.V. Moore, H.A. Hopkins and W.B. Looney (1980) Dynamic histology of a rat hepatoma and the response to 5-fluorouracil. *Cell Tissue Kinet.* **13**, 53-63.

27. J.V. Moore, H.A. Hopkins and W.B. Looney (1983) Response of cell populations in tumor cords to a single dose of cyclophosphamide or radiation. *Eur. J. Cancer Clin. Oncol.* **19**, 73-79.

28. J.V. Moore, H.A. Hopkins and W.B. Looney (1984) Tumour-cord parameters in two rat hepatomas that differ in their radiobiological oxygenation status. *Radiat. Environ. Biophys.* **23**, 213-222.

29. J.V. Moore, P.S. Hasleton and C.H. Buckley (1985) Tumour cords in 52 human bronchial and cervical squamous cell carcinomas: Inferences for their cellular kinetics and radiobiology. *Br. J. Cancer* **51**, 407-413.

30. S.I. Rubinow (1968) A maturity-time representation for cell populations. *Biophys. J.* **8**, 1055-1073.

31. I.F. Tannock (1968) The relation between cell proliferation and the vascular system in a transplanted mouse mammary tumour. *Br. J. Cancer* **22**, 258-273.

28.

32. I. Tannock, and A. Howes (1973) The response of viable tumor cords to a single dose of radiation. *Radiat. Res.* **55**, 477-486.

33. G.F. Webb (2002) The steady state of a tumor cord cell population. *J. Evolut. Equat.*, in press.